Article:
Sng, CCT, O'Byrne, S, Prigozhin, DM et al. (16 more authors) (2018) A Type III Complement Factor D Deficiency: Structural insights for inhibition of the alternative pathway. Journal of Allergy and Clinical Immunology, 142 (1). 311-314.e6. ISSN 0091-6749

https://doi.org/10.1016/j.jaci.2018.01.048

Accepted Manuscript

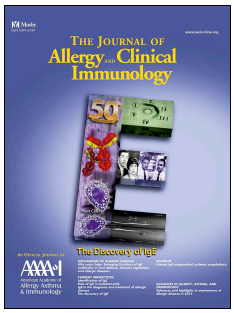

A Type III Complement Factor D Deficiency: Structural insights for inhibition of the alternative pathway

Christopher C.T. Sng, MB BChir, Sorcha O'Byrne, BSc, Daniil M. Prigozhin, PhD, Matthias R. Bauer, PhD, Jennifer C. Harvey, BSc, Michelle Ruhle, BBiomedSc, Ben G. Challis, PhD, Sara Lear, MBBS, Lee D. Roberts, PhD, Sarita Workman, RN MSc, Tobias Janowitz, PhD, Lukasz Magiera, PhD, Rainer Doffinger, PhD FRCPath, Matthew S. Buckland, PhD FRCPath, Duncan J. Jodrell, DM MSc FRCP, Robert K. Semple, MB PhD, Timothy J. Wilson, PhD, Yorgo Modis, PhD, James E.D. Thaventhiran, PhD FRCPath

PII: S0091-6749(18)30327-0

DOI: 10.1016/j.jaci.2018.01.048

Reference: YMAI 13343

To appear in: *Journal of Allergy and Clinical Immunology*

Received Date: 24 October 2017

Revised Date: 2 January 2018

Accepted Date: 16 January 2018

Please cite this article as: Sng CCT, O'Byrne S, Prigozhin DM, Bauer MR, Harvey JC, Ruhle M, Challis BG, Lear S, Roberts LD, Workman S, Janowitz T, Magiera L, Doffinger R, Buckland MS, Jodrell DJ, Semple RK, Wilson TJ, Modis Y, Thaventhiran JED, A Type III Complement Factor D Deficiency: Structural insights for inhibition of the alternative pathway, *Journal of Allergy and Clinical Immunology* (2018), doi: 10.1016/j.jaci.2018.01.048.

TITLE PAGE

Letter to the Editor

A Type III Complement Factor D Deficiency: Structural insights for inhibition of the alternative pathway.

Christopher C. T. Sng, MB BChir,[1*] Sorcha O'Byrne, BSc,[2*] Daniil M. Prigozhin, PhD[3*], Matthias R. Bauer, PhD,[4*] Jennifer C. Harvey, BSc,[5] Michelle Ruhle, BBiomedSc,[6] Ben G. Challis, PhD,[7] Sara Lear, MBBS,[2] Lee D. Roberts, PhD,[9] Sarita Workman, RN MSc,[5] Tobias Janowitz, PhD,[1] Lukasz Magiera, PhD,[1] Rainer Doffinger, PhD FRCPath,[2] Matthew S. Buckland, PhD FRCPath,[5] Duncan J. Jodrell, DM MSc FRCP,[1] Robert K. Semple, MB PhD,[7] [8] Timothy J. Wilson, PhD,[10] Yorgo Modis, PhD,[3] James E. D. Thaventhiran, PhD FRCPath.[1] [2 11 12]

[1]Cancer Research UK Cambridge Institute, Robinson Way, Cambridge, CB2 0RE U.K.

[2]Department of Clinical Immunology, Cambridge University Hospitals NHS Trust, Addenbrooke's Hospital, Cambridge, CB2 0QQ U.K.

[3]Molecular Immunity Unit, Department of Medicine, MRC Laboratory of Molecular Biology, Cambridge Biomedical Campus, Francis Crick Ave, Cambridge CB2 0QH, U.K.

[4] MRC Laboratory of Molecular Biology, Cambridge Biomedical Campus, Francis Crick Ave, Cambridge CB2 0QH, U.K.

[5]Department of Immunology, Royal Free London NHS Foundation Trust, Pond Street, Hampstead, London, NW3 2QG U.K.

[6]The Walter and Eliza Hall Institute of Medical Research, 1G Royal Parade, Parkville, Victoria, Australia 3058

[7]Wellcome Trust-MRC Institute of Metabolic Science, Addenbrooke's Hospital, Cambridge, CB2 0QQ U.K.

[8]University of Edinburgh Centre for Cardiovascular Sciences, Queen's Medical Research Institute, Little France Crescent, Edinburgh EH16 4TJ.

[9]Leeds Institute of Cardiovascular and Metabolic Medicine, LIGHT Laboratories University of Leeds, LS2 9JT U.K.

[10]Department of Microbiology, Miami University, 68 Pearson Hall, 700 E. High Street, Oxford, OH 45056 U.S.A.

[11]Department of Medicine, University of Cambridge, Addenbrooke's Hospital, Cambridge, CB2 0QQ U.K.

[12]MRC Toxicology Unit, Hodgkin Building, University of Leicester, LE1 9HN U.K.

* These authors contributed equally to this work.

Corresponding author

James E. D. Thaventhiran, PhD

Department of Medicine

Addenbrooke's Hospital

Box 157

Hills Rd

Cambridge

CB2 0QQ U.K.

Telephone: +44 7740 703599

Fax: +44 1223 336846

E-mail: jedt2@cam.ac.uk

Declaration of all sources of funding: JEDT is supported by an MRC Clinician Scientist Fellowship (MR/L006197/1). This work was funded by BRC III PPG funding and a Wellcome Trust Senior Research Fellowship to Y.M. (101908/Z/13/Z). RKS is funded by the Wellcome Trust [grant number WT098498 and strategic award 100574/Z/12/Z], the United Kingdom Medical Research Council [MRC_MC_UU_12012/5] and the United Kingdom National Institute for Health Research (NIHR) Cambridge Biomedical Research Centre. TJ is funded by Cancer Research UK (Clinician Scientist Fellowship C42738/A24868). BGC is now a full-time employee of Astra-Zeneca.

Word count: 1012

Capsule summary

We fully characterise the first reported functional deficiency of complement factor D in a patient. The structural analysis yielded a novel approach by which this key enzyme could be inhibited to treat inflammatory diseases.

Key words

Adipsin, age-related macular degeneration, alternative pathway, complement deficiency, complement serine protease, drug development, factor D, glucose homeostasis, single-nucleotide variant, type III deficiency

Abbreviations used

AMD: age-related macular degeneration

AP: alternative complement pathway

AP50: alternative pathway haemolytic activity

CH50: classical pathway haemolytic activity

FB: complement factor B

FD: complement factor D

MD: molecular dynamics

WT: wild-type

To the Editor:

We investigated an alternative complement pathway (AP) deficiency in a patient with absent alternative pathway haemolytic activity (AP50) but normal classical pathway haemolytic activity recovering from invasive meningococcal infection (for patient and sibling details, see Appendix A in this article's Online Repository). Serum reconstitution with proximal AP components suggested a Factor D (FD) deficiency (Fig 1A). Sanger sequencing of *CFD* identified a rare homozygous missense mutation (c.602G>C) in exon 4 in the patient (II-1) and sibling (II-2), resulting in an arginine to proline substitution (p. R176P) (see Fig E1, A, in this article's Online Repository). This genotype co-segregated with an AP50-null phenotype, as the parents, both heterozygotes, had normal AP50 (Fig 1B). In contrast to previous confirmed FD deficiencies,[1-3] all members of the pedigree had normal levels of circulating FD, as corroborated by western blot (see Fig E1, B). Meanwhile, identical circular dichroism spectra and melting curves of recombinant wild-type (WT) and R176P FD precluded gross changes in FD structure or stability, suggesting a functional deficiency (Fig 1C and see Fig E1, C). We assessed the cleavage of C3b-bound Factor B (FB) by recombinant WT and mutant FD (R176P, R176A, R176Q). WT FD could cleave C3b-bound FB to produce fragments Bb and Ba. Conversely, R176P FD demonstrated diminished *in vitro* catalytic activity at all concentrations, and had negligible activity at physiological concentration (0.04 μM) (Fig 1D and see E1, D). Reconstitution of FD-depleted serum with R176P FD also demonstrated impaired AP mediated haemolysis (see Fig E1, E).

FD's serine protease activity depends on obligatory binding to the C3bB complex via four exosite loops (residues 132-135, 155-159, 173-176, 203-209). This leads to rearrangement of the self-inhibitory loop (199-202), allowing realignment of His41 and Asp89 with Ser183 to form the active catalytic triad (see Fig E2, A and B, in this article's Online Repository).[4, 5]

Mutation R176P lies outside the active site, within one of the FB-binding exosite loops. We used molecular dynamics (MD) stimulations to study how the R176P mutation affects the FD protein fold (see Fig E2, C). In mutant FD, we observed a rearrangement of the exosite loop 155-161 within 50 ns of simulation (Fig 2A). This was unexpected because loop 155-161 was not in direct contact with residue 176. Average structures generated from the final 50 ns of simulation for WT and mutant FD (R176P and R176A) demonstrated that key FB-binding residues Asp161 and Arg157 were shifted by 4.3 Å and 1.9 Å respectively (Cα average position) (Fig 2B). Superimposing these MD average structures onto the crystal structure of the C3bB-D complex revealed that Asp161 and Arg157 assumed a conformation that no longer supported binding due to loss of shape and charge complementarity to the FB surface (Fig 2C). The other three exosite loops retained their binding-competent conformations. After assuming the new conformation, exosite loop 155-161 demonstrated higher conformational mobility (root mean square fluctuation) relative to WT (Fig E2, D and E). In contrast, the mobility of loops containing catalytic residues His41 and Asp89 decreased in the mutants. Using the distance between His41 and Ser183 during MD simulations as a proxy for the active site conformation, we observed that WT could sample the short distance necessary for a catalytically active conformation (Fig 2D). Conversely, in both mutant simulations, the distance remained larger, consistent with His41 pointing away from the active site. Therefore, in addition to disruption of key FB-binding residues, mutations R176P and R176A appear to stabilise the self-inhibited conformation of free FD.

To assess the binding of FD to C3bB, we used surface plasmon resonance. Co-injection of catalytically inactive FD (WT/S183A) with FB demonstrated a dose-dependent increase in binding to C3b and complex formation (Fig 2E). In contrast, R176P/S183A FD lacked any detectable binding (Fig 2F). Consistent with the stochastic transitions of free WT FD to the

active conformation observed in the MD simulation, FD has a low level of esterolytic activity towards a small synthetic substrate, Z-Lys-SBzl (Fig 2D). Surprisingly, R176P FD demonstrated a loss of esterolytic activity similar to the active site mutant, S183A (see Fig 2G).

Deficiency of properdin, the most common AP deficiency, can result from absent (type I), low (type II) or normal but non-functioning (type III) protein levels (for reference, see Reference E10 in this article's Online Repository). Meanwhile, previously confirmed deficiencies of activating complement serine proteases have all resulted in low or absent gene product. We have identified a unique deficiency: R176P FD is fully expressed and stable, but enzymatically inert, constituting a functional or Type III deficiency. Recent preclinical evidence[6] that FD deficient mice are susceptible to diabetes prompted metabolic assessment in the FD deficient patients. No abnormality was detected (for details, see Appendix B, Fig E3 and Table E1 in this article's Online Repository).

Over-activation of AP is implicated in numerous inflammatory disorders, including age-related macular degeneration (AMD). Therefore, blockade of the AP by targeting the rate-limiting enzyme, FD, is an attractive approach to controlling disease progression. An anti-FD Fab fragment targeting the two distal exosite loops has shown some benefit in phase II clinical trials for treatment of dry AMD.[7] *In vitro* studies indicate that it inhibits binding to the C3bB complex but *increases* esterolytic activity towards small-molecule substrates.[8] This may result in unwanted clinical effects due to non-specific activity or limit its efficacy *in vivo*. In the case of R176P FD, both FB-binding *and* esterolytic activity are abrogated through exosite hindrance and stabilisation of the self-inhibited state. Loop 173-176 is thus a promising target for allosteric inhibitors of FD that stabilise the inhibitory loop in addition to

binding-blockade. A structure-based design approach to targeting FD has recently succeeded in identifying candidate FD inhibitors where high-throughput screens had failed,[9] highlighting the benefits of integrating structural information into candidate drug screens. Comprehensive definition of the structural and molecular determinants of *in vivo* FD activity is critical for this. This study of the R176P mutation demonstrates how in-depth mechanistic analysis of rare complement deficiencies can deliver such insight validated clinically by *in vivo* human evidence of AP blockade.

Our acknowledgements can be found in this article's Online Repository.

Christopher C. T. Sng, MB BChir[1*]
Sorcha O'Byrne, BSc[2*]
Daniil M. Prigozhin, PhD[3*]
Matthias R. Bauer, PhD[4*]
Jennifer C. Harvey, BSc[5]
Michelle Ruhle, BBiomedSc[6]
Ben G. Challis, PhD[7]
Sara Lear, MBBS[2]
Lee D. Roberts, PhD[9]
Sarita Workman, RN MSc[5]
Tobias Janowitz, PhD[1]
Lukasz Magiera, PhD[1]
Rainer Doffinger, PhD FRCPath[2]
Matthew S. Buckland, PhD FRCPath[5]
Duncan J. Jodrell, DM MSc FRCP[1]

Robert K. Semple, MB PhD[7 8]

Timothy J. Wilson, PhD[10]

Yorgo Modis, PhD[3]

James E. D. Thaventhiran, PhD FRCPath[1 2 11 12]

From [1]Cancer Research UK Cambridge Institute, Cambridge, United Kingdom; [2]Department of Clinical Immunology, Cambridge University Hospitals NHS Trust, Addenbrooke's Hospital, Cambridge, United Kingdom; [3]Molecular Immunity Unit, Department of Medicine, MRC Laboratory of Molecular Biology, Cambridge, United Kingdom; [4]MRC Laboratory of Molecular Biology, Cambridge, United Kingdom; [5]Department of Immunology, Royal Free London NHS Foundation Trust, London, United Kingdom; [6]The Walter and Eliza Hall Institute of Medical Research, Parkville, Victoria, Australia; [7]Wellcome Trust-MRC Institute of Metabolic Science, Addenbrooke's Hospital, Cambridge, United Kingdom; [8]University of Edinburgh Centre for Cardiovascular Sciences, Queen's Medical Research Institute, Little France Crescent, Edinburgh EH16 4TJ; [9]Leeds Institute of Cardiovascular and Metabolic Medicine, LIGHT Laboratories, University of Leeds, Leeds, United Kingdom; [10]Department of Microbiology, Miami University, Oxford, United States of America; [11]Department of Medicine, University of Cambridge, Addenbrooke's Hospital, Cambridge, United Kingdom; and the [12]MRC Toxicology Unit, Hodgkin Building, University of Leicester, LE1 9HN United Kingdom.

* These authors contributed equally to this work.

205 **References**

206 1. Hiemstra PS, Langeler E, Compier B, Keepers Y, Leijh PC, van den Barselaar MT, et
207 al. Complete and partial deficiencies of complement factor D in a Dutch family. J
208 Clin Invest 1989; 84:1957-61.
209 2. Biesma DH, Hannema AJ, van Velzen-Blad H, Mulder L, van Zwieten R, Kluijt I, et
210 al. A family with complement factor D deficiency. J Clin Invest 2001; 108:233-40.
211 3. Sprong T, Roos D, Weemaes C, Neeleman C, Geesing CL, Mollnes TE, et al.
212 Deficient alternative complement pathway activation due to factor D deficiency by 2
213 novel mutations in the complement factor D gene in a family with meningococcal
214 infections. Blood 2006; 107:4865-70.
215 4. Narayana SV, Carson M, el-Kabbani O, Kilpatrick JM, Moore D, Chen X, et al.
216 Structure of human factor D. A complement system protein at 2.0 A resolution. J Mol
217 Biol 1994; 235:695-708.
218 5. Forneris F, Ricklin D, Wu J, Tzekou A, Wallace RS, Lambris JD, et al. Structures of
219 C3b in complex with factors B and D give insight into complement convertase
220 formation. Science 2010; 330:1816-20.
221 6. Lo JC, Ljubicic S, Leibiger B, Kern M, Leibiger IB, Moede T, et al. Adipsin is an
222 adipokine that improves beta cell function in diabetes. Cell 2014; 158:41-53.
223 7. Yaspan BL, Williams DF, Holz FG, Regillo CD, Li Z, Dressen A, et al. Targeting
224 factor D of the alternative complement pathway reduces geographic atrophy
225 progression secondary to age-related macular degeneration. Sci Transl Med 2017; 9.
226 8. Katschke KJ, Jr., Wu P, Ganesan R, Kelley RF, Mathieu MA, Hass PE, et al.
227 Inhibiting alternative pathway complement activation by targeting the factor D
228 exosite. J Biol Chem 2012; 287:12886-92.

9. Maibaum J, Liao SM, Vulpetti A, Ostermann N, Randl S, Rudisser S, et al. Small-molecule factor D inhibitors targeting the alternative complement pathway. Nat Chem Biol 2016; 12:1105-10.

234 **Figure legends**

235 **Figure 1:** Assessing the contribution of mutation R176P to AP dysfunction.

236 (A) AP50 assay assessing patient serum supplemented with properdin (P), factor B (FB) or

237 factor D (FD).

238 (B) The immediate family pedigree of the patient with the *CFD* genotype, serum AP50 and

239 serum FD concentrations displayed. *D*, WT allele. *d*, mutant allele (c.602G>C).

240 (C) Thermal shift assay of WT and R176P FD.

241 (D) Serial dilutions of recombinant WT or R176P FD were incubated with C3b and FB. The

242 SDS-PAGE gel, stained with AcquaStain, shows the individual proteins and resultant

243 products.

244

245 **Figure 2:** Defining the effects of the R176P mutation on FD function.

246 (A and B) FB-binding exosite loop 155-167 assumes a new conformation in mutant FD

247 simulation. Arrows highlight average Cα position shifts of two residues that bind C3bB in the

248 R176P FD simulation.

249 (C) Loss of shape complementarity at the FD-C3bB interface. FD exosite loops from

250 published co-crystal structures (white, PDB ID: 2XWB) overlaid with the simulated loops of

251 WT and mutant FD.

252 (D) Distance sampled between the active site Nε2 nitrogen of His41 and Oγ of Ser183 during

253 each simulation. The shorter distance is necessary for catalytic activity.

254 (E and F) SPR binding measurement of enzymatically inactive recombinant FD

255 (R176P/S183A or WT/S183A) to C3bB complex.

256 (G) Steady state kinetics for Z-Lys-SBzl cleavage by WT, R176P, R176A and catalytically

257 inactive control S183A FD.

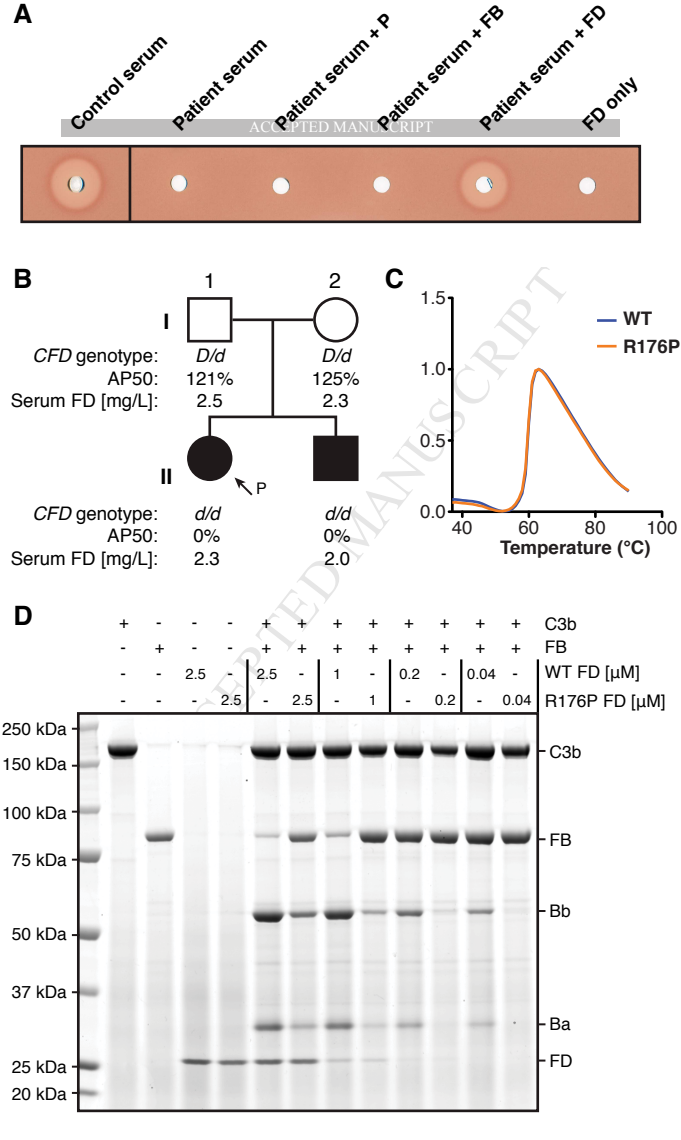
A
Control serum
Patient serum
Patient serum + P
Patient serum + FB
Patient serum + FD
FD only
B
1
2
I
CFD genotype:
D/d
D/d
AP50:
121%
125%
Serum FD [mg/L]:
2.5
2.3
II
P
CFD genotype:
d/d
d/d
AP50:
0%
0%
Serum FD [mg/L]:
2.3
2.0
C
1.5
1.0
0.5
0.0
40
60
80
100
Temperature (°C)
WT
R176P
D
C3b
FB
WT FD [μM]
R176P FD [μM]
250 kDa
150 kDa
100 kDa
75 kDa
50 kDa
37 kDa
25 kDa
20 kDa
C3b
FB
Bb
Ba
FD

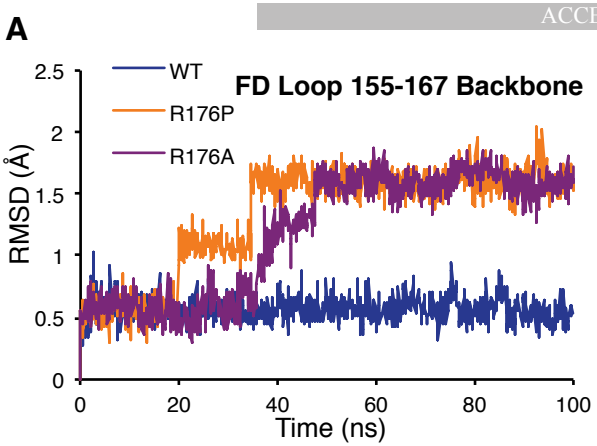

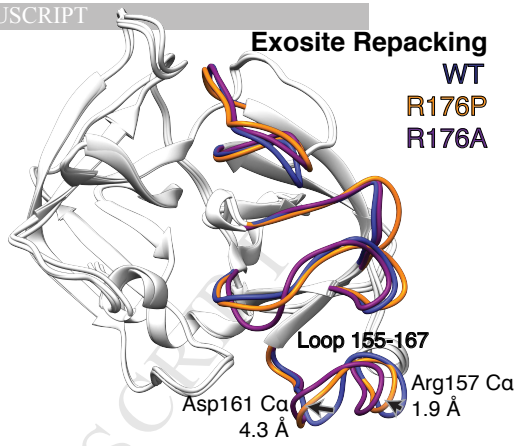

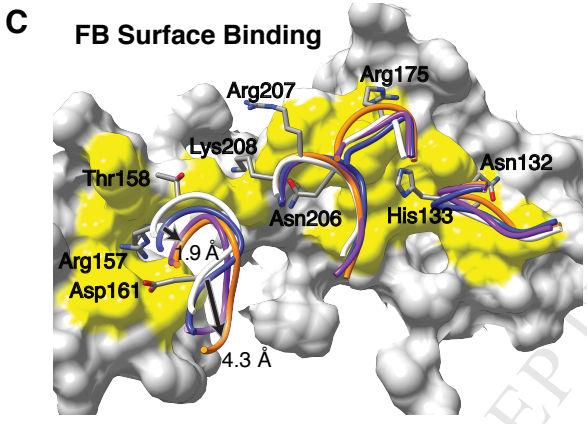

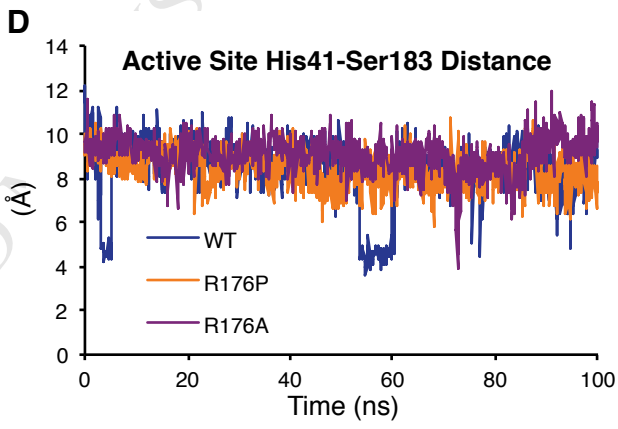

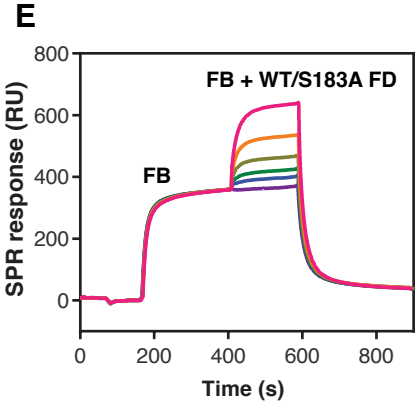

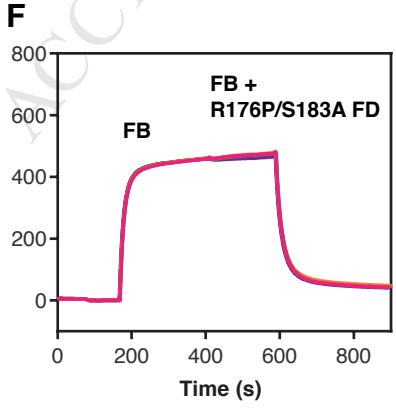

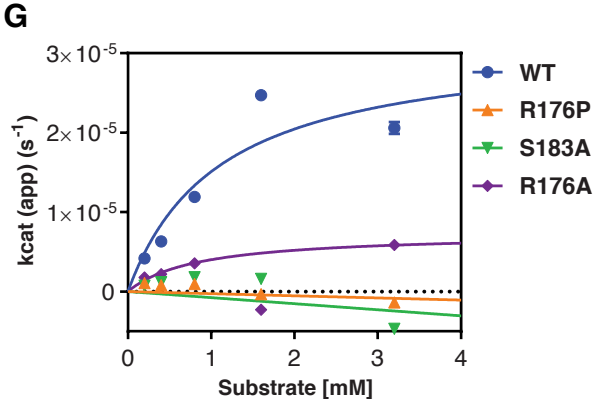

APPENDIX A

Patient details

A 19-year-old, South Asian female presented with a 24-hour history of high fever, rigors, delirium and diarrhoea. On clinical examination, she was febrile with a purpuric rash and a reduced level of consciousness (Glasgow Coma scale score: 9/15). Intravenous antibiotic therapy was initiated for provisionally diagnosed meningococcal septicaemia. She was intubated and transferred to the intensive care unit where she developed disseminated intravascular coagulation, for which she received treatment. Results from blood cultures drawn at the time of admission confirmed an infection with Neisseria meningitides serogroup Y. Her clinical condition improved with intensive care support and antimicrobial therapy. She was discharged after two weeks with minimal sequelae including bilateral leg scarring, a sacral pressure sore and mild bilateral hearing loss.

At the age of 5 years, she had received bilateral tympanostomy tubes for recurrent ear infections and otitis media with effusion but had no other unusual infections as a child. She received the full course of childhood vaccinations as per the national immunisation schedule.

On screening for immunodeficiency, laboratory measurement demonstrated a normal full blood count with normal counts of lymphoid cells. The titres of C3, C4, mannose-binding lectin and C1q were within normal range, but there was undetectable alternative pathwayhaemolytic activity (AP50) in conjunction with normal classical pathway haemolytic activity. In view of her complement deficiency, she was prescribed lifelong phenoxymethylpenicillin as antimicrobial prophylaxis. She was also vaccinated for meningitis ACWY, meningitis C, pneumococcus and haemophilus influenza B to which she developed high antibody titre responses.

Her sole sibling, a younger male, who was homozygous for the same mutation, leading to an identical pattern on immunodeficiency screening, was healthy at assessment. He reported no excess of infections in the past. Of note, he reported having been treated empirically for suspected meningitis, aged 11, whilst travelling in Mauritius from which he recovered with no sequalae after a standard course of antibiotics.

APPENDIX B

Functional Factor D deficiency does not result in impaired oral glucose tolerance

Recent pre-clinical evidence[E1] that FD regulates insulin secretion prompted metabolic assessment of the patient and her sibling. They had a BMI of 19.3 kg/m^2 and 23.1 kg/m^2, respectively. Fasting venous plasma glucose (5.2-5.4 mmol/L) and insulin (29-39 pmol/L) levels were normal in both subjects (Fig E3). Similarly, plasma glucose excursions were normal in response to an oral glucose (75g) challenge. At 120 minutes following glucose administration, glucose levels remained normal (4.0 mmol/L). Furthermore, circulating concentrations of leptin and adiponectin, adipokines which regulate insulin sensitivity, were normal, as were fasting lipid profiles in both subjects. Thus, glucose homeostasis is not impaired in the context of genetic, and therefore lifelong, FD deficiency.

These results are consistent with the finding that FD knock-out mice developed impaired glucose tolerance only on a long-term diabetogenic diet. This suggests that FD may contribute little to glucose homeostasis in the absence of prolonged metabolic stress. Alternatively, the role of FD in glucose homeostasis could be independent of binding to C3bB or independent of its serine protease activity and, by extension, independent of its downstream effects on the complement cascade. While congenital deficiency of FD alone

may not lead to insulin insufficiency, Lo et al.'s findings warrant observation of oral glucose tolerance in such FD deficient patients under extreme metabolic stress and at older age. Further research will be required to understand the role of FD in glucose homeostasis and FD-deficient family pedigrees offer a useful clinical insight to this question.

METHODS

Informed consent statement

All study participants gave their informed consent as appropriate under approved protocols from local institutional review boards. The research was conducted at University College London and the University of Cambridge under approved protocols (#04/Q0501/119 for affected individuals, #07/H0720/182 for family members).

Alternative pathway haemolytic activity measurement

AP100 RC003.1 Kit (Binding Site) agar-chicken erythrocyte plates were prepared according to the manufacturer's instructions, with kit control and calibration solutions added. 5µl aliquots of test serum were added to individual wells on the plates over ice. The loaded plates were then stored at 4°C for 18 hours to allow radial diffusion of serum components, followed by incubation at 37°C for 90 minutes to develop zones of lysis. The plates were then digitally scanned at high-resolution, and the diameters of zones of lysis were measured using ImageJ 1.x computer software. Representative plates were selected for figures. The diameter of lysis correlates with alternative pathway activity (AP50) and is expressed out of 100% relative to kit control. Purified human Factor D (FD), Factor B and properdin for reconstitution assays were purchased from Complement Tech, Inc.

Sanger sequencing

Genomic DNA was isolated from blood samples with QIAamp Kits (QIAGEN). The *CFD* gene polymerase chain reaction was performed with primers annealing to intron sequences close to each exon as described previously[E2]. Specifically, regarding the R176P mutation, a 258-bp genomic fragment comprising exon 4 was amplified by PCR with the primers 5'-CTGGGGCATAGTCAACCAC-3' and 5'-TGGGCCCTGTTCCTACTTG-3'. The cDNA

numbering for the *CFD* variant identified is based on transcript NCBI Ref Seq accession no. NM_001928/Ensembl accession no. ENST00000327726.6, beginning at the ATG start codon. The genomic coordinates refer to the GRCh37 genome build.

Western blot analysis

Pooled control and the patient serum were diluted to 1:40 in tris-buffered saline and resolved by SDS-PAGE on NuPAGE 4-12% Bis-Tris Gels, then blotted to nitrocellulose membranes. FD was detected using goat anti-human FD (AF1824; R&D) and donkey anti-goat-IgG IRDye 680CW (LI-COR Biosciences, Lincoln, NE, USA) secondary antibodies. The membranes were imaged using the Odyssey Infrared Imaging System (LI-COR Biosciences, Nebraska, USA)

Recombinant CFD expression and purification

Lentiviral transfer plasmid, envelope plasmid (pMD2.G; gift from Didier Trono; AddGene plasmid #12260) and packaging plasmid (psPAX2; AddGene; gift from Didier Trono; AddGene plasmid #12259) were used to transfect HEK293T cells to produce lentiviral particles. The transfer vector (modified pLenti-CMV-GFP-Puro; gift of Eric Campeau – Addgene 17448) included human FD cDNA (WT, R176P, R176A, S183A) with C-terminus hexahistidine tag upstream of an IRES-Thy1.1 and a puromycin resistance gene ($Puro^R$). Transfection was carried out using Lipofectamine 3000 and, after 24hrs, the media containing the lentiviral particles was used immediately to stably transduce newly plated HEK293T cells. After puromycin selection, stably transduced 293T cells were incubated with FreeStyle media (Gibco) supplemented with 6X Glutamax and 2mM valproic acid. After 7-14 days, secreted recombinant CFD was purified from this media using cobalt immobilised metal affinity chromatography. CFD was eluted in 150mM imidazole in PBS and buffer exchanged

by centrifugal concentration (Vivaspin® 20; 10,000Da pore size; Sartorius). Purity of the sample was confirmed on SDS-PAGE and mass spectrometry.

Measuring *in vitro* catalytic activity of recombinant FD

Purified human C3b and FB were purchased from Complement Technology, Inc. Recombinant WT, R176P or R176A FD were mixed in varying concentrations (1.0 μM, 0.2 μM, 0.04 μM) with C3b (1.0 μM) and FB (1.0 μM) in veronal buffer (Lonza) with 10 mM $MgCl_2$ to a final volume of 20 μL. Reaction tubes were incubated for 10 minutes at 37°C before the addition of sample loading buffer (NuPAGE® LDS Sample Buffer) to terminate the reaction. The samples were then heated to 70°C for 10 minutes and resolved by SDS-PAGE on a Novex NuPAGE 4-12% Bis-Tris Gel. The gels were developed overnight with AcquaStain (Bulldog Bio), washed for 1 hour with distilled water, dried and digitally scanned at high-resolution. Analysis of percentage cleavage of FB was calculated by densitometry analysis using ImageJ 1.x computer software. Statistical comparisons between WT and R176P FD activity were performed at each concentration, from 4 independent experiments using the Kruskall-Wallis non-parametric t-test.

Circular dichroism spectroscopy and thermal shift assay

WT and R176P catalytically inactive (S183A) proteins were purified by size exclusion chromatography in chloride-free 0.1M sodium phosphate pH 7.0, diluted to a concentration of 2 mg/mL (72.4 μM), and loaded into a 0.1 mm quartz sample cell. Circular dichroism spectra were recorded at 20°C on a Jasco J-810 spectropolarimeter equipped with a Jasco PTC-348WI temperature controller. Spectra were acquired from 190-260 nm with 0.1 nm resolution and 1 nm bandwidth. Final spectra are the sum of 20 scans acquired at 50 nm/minute. **Thermal shift assay.** 2 μg of protein was mixed with SYPRO Orange in PBS

with 25mM HEPES and fluorescence data acquired on a ViiA 7 real-time PCR system with thermal denaturation over increasing temperatures observed using 1°C intervals.

Molecular dynamics (MD) simulation of mutant FD

Starting models were derived from crystal structures of S183A FD (PDB ID 2XW9, 1.2 Å resolution) reported previously.[E3] The catalytic residue was reverted to serine during the MD setup. Coot[E4] was used to place the Pro176 side chain in the Arg176 experimental density while minimizing clashes with surrounding atoms and aiming to achieve a favourable initial geometry. The resulting structures were further adjusted in UCSF Chimera.[E5] The GROMACS package[E6] was used to set up and run MD simulations. The AMBER99SB-ILDN force field[E7] and TIP3P water model were used and the structures placed in dodecahedral boxes with 10 Å padding and surrounded with solvent including water and 150 mM NaCl. Following steepest gradient energy minimization, a modified Berendsen thermostat (two groups, time constant 0.1 ps, temperature 310 K) followed by a Berendsen barostat (isotropic, coupling constant 0.5 ps, reference pressure 1 bar) were coupled to the system over 100 ps. 100 ns runs of unrestrained MD trajectories were produced. Following removal of periodic boundary condition artefacts, MD runs were visualised and analysed in Chimera and bulk statistics extracted using GROMACS analysis routines.

Surface plasmon resonance

Binding experiments were carried out based on established protocol using a Biacore T200 instrument.[E8] FB and FD were buffer exchanged by gel filtration into veronal buffer with 10mM $MgCl_2$. C3b was immobilised on the CM5 chip by amine coupling to achieve 8000 resonance units. A dual injection programme was designed where 0.1 μM or 1 μM FB was injected at a flow rate of 30uL/min for 3 minutes, followed by a second injection of a mix of

0.1 μM or 1 μM FB and FD at 30uL/min for 4 minutes. After 5 minutes for dissociation, the chip was regenerated by three 5-minute washes in 40mM acetate + 3M NaCl (pH 5.5). The chip was re-equilibrated in assay buffer for 5 minutes. Catalytically inactive FD (S183A) or double mutant R176P/S183A were used to emulate the binding response of wild-type or R176P respectively while preventing cleavage of FB and subsequent dissociation of the complex.

Esterolytic activity of FD

Z-Lys-SBzl was purchased from Sigma-Aldrich in powder form and reconstituted to 100 mM in 70% DMSO. The assay buffer consisted of 50 mM HEPES (pH7.5), 220mM NaCl and 2 mM of Ellman's reagent (5,5-dithio-bis-(2-nitrobenzoic acid) [DTNB]; Sigma-Aldrich). Each reaction mixture contained FD (80nM), variable Z-Lys-SBzl concentrations (0.2-3.2 mM) and 8% v/v of DMSO in a final volume of 200 μl. Solutions were pre-warmed to 37°C before addition of substrate to initiate the reaction. Hydrolysis of Z-lys-SBzl was measured using CLARIOstar FS microplate reader through equimolar formation of chromophore 2-nitro-5-thiobenzoate at 405 nm every 30 seconds for 90 minutes (ε = 13,600 $M^{-1}cm^{-1}$). The rate of hydrolysis was determined from linear slopes of the reaction curves. Reaction velocities, expressed in apparent turnover values were plotted against substrate concentration.

Table E1

Analyte	Proband	Sibling
Leptin (ng/ml)	10.6	11.3
Adiponectin (μg/ml)	9.7	6.5
NEFA (μmol/L)	391	212
Cholesterol (mmol/L)	4.2	4
HDL (mmol/L)	1.53	1.26
LDL (mmol/L)	2.3	2.3
Triglycerides (mmol/L)	0.8	0.9
HbA1c (mmol/mol)	36	35

NEFA, non-esterified fatty acids. *HDL*, high-density lipoprotein. *LDL*, low-density lipoprotein.

177 **References**

178 E1. Lo JC, Ljubicic S, Leibiger B, Kern M, Leibiger IB, Moede T, et al. Adipsin is an
179 adipokine that improves beta cell function in diabetes. Cell 2014; 158:41-53.
180 E2. Sprong T, Roos D, Weemaes C, Neeleman C, Geesing CL, Mollnes TE, et al.
181 Deficient alternative complement pathway activation due to factor D deficiency by 2
182 novel mutations in the complement factor D gene in a family with meningococcal
183 infections. Blood 2006; 107:4865-70.
184 E3. Forneris F, Ricklin D, Wu J, Tzekou A, Wallace RS, Lambris JD, et al. Structures of
185 C3b in complex with factors B and D give insight into complement convertase
186 formation. Science 2010; 330:1816-20.
187 E4. Emsley P, Lohkamp B, Scott WG, Cowtan K. Features and development of Coot.
188 Acta Crystallogr D Biol Crystallogr 2010; 66:486-501.
189 E5. Pettersen EF, Goddard TD, Huang CC, Couch GS, Greenblatt DM, Meng EC, et al.
190 UCSF Chimera--a visualization system for exploratory research and analysis. J
191 Comput Chem 2004; 25:1605-12.
192 E6. Abraham MJ, Murtola T, Schulz R, Pall S, Smith JC, Hess B, et al. GROMACS: High
193 performance molecular simulations through multi-level parallelism from laptops to
194 supercomputers. SoftwareX 2015; 1-2:19-25.
195 E7. Lindorff-Larsen K, Piana S, Palmo K, Maragakis P, Klepeis JL, Dror RO, et al.
196 Improved side-chain torsion potentials for the Amber ff99SB protein force field.
197 Proteins 2010; 78:1950-8.
198 E8. Katschke KJ, Jr., Wu P, Ganesan R, Kelley RF, Mathieu MA, Hass PE, et al.
199 Inhibiting alternative pathway complement activation by targeting the factor D
200 exosite. J Biol Chem 2012; 287:12886-92.

E9. Lek M, Karczewski KJ, Minikel EV, Samocha KE, Banks E, Fennell T, et al. Analysis of protein-coding genetic variation in 60,706 humans. Nature 2016; 536:285-91.

E10. Fredrikson GN, Westberg J, Kuijper EJ, Tijssen CC, Sjoholm AG, Uhlen M, et al. Molecular characterization of properdin deficiency type III: dysfunction produced by a single point mutation in exon 9 of the structural gene causing a tyrosine to aspartic acid interchange. J Immunol 1996; 157:3666-71.

Figure legends

Figure E1: Mutation R176P results in a type III FD deficiency.

(A) Chromatograms for the DNA sequence adjacent to position c.602 are shown for each member of the pedigree. The identified variant is rare: the EXAC database reports mutation R176P (variant 19:861943 G/C) at an allele frequency of $1.049x10^{-4}$, with no homozygotes.[E9]

(B) Western blot analysis of FD in serum from the patient and healthy control.

(C) Secondary structural compositions of WT and R176P FD were evaluated using circular dichroism spectroscopy.

(D) Comparison of *in vitro* catalytic activity of recombinant WT, R176P, R176Q and R176A FD in terms of FB cleavage. (***, p<.001; ****, p<.0001).

(E) Recombinant WT and R176P FD were tested for the ability to reconstitute alternative pathway haemolytic activity when added to FD-depleted serum.

Figure E2: Mutation R176P stabilises the self-inhibited state of FD.

(A) Structure of free FD[E3] (PDB ID: 2XW9) showing the catalytic triad (Ser183-His41-Asp89) in an inactive conformation stabilised by the self-inhibitory loop 199-202 (red) and an ion bridge between Asp177 and Agr202. The exosite loops are shown in yellow.

(B) Structure of C3bB-bound FD[E3] (PDB ID: 2XWB) omitting the C3b and FB components. FD exosite loops retain a conformation similar to that of unbound FD.

(C) WT, R176P and R176A structures were stable over 100 ns of unrestrained molecular dynamics simulation with explicit solvent. *RMSD*, root mean square deviation.

(D) Root mean square fluctuation (RMSF) in WT and mutant FD over the second half of the trajectory.

(E) Differences in WT versus R176 RMSF mapped to the FD structured. MD predicted increased mobility in exosite loops, notably 155-167, and decreased mobility in loops carrying the catalytic His41 and Asp89 residues.

Fig E3: Assessment of glucose tolerance in patients with functional FD deficiency. Patient and sibling were given 75g of oral glucose at 0 minutes and blood glucose was measured at regular intervals between 0 - 120 minutes. The error bars indicate the range of plasma glucose concentrations between the patient and sibling.